Biomed Microdevices (2009) 11:1269–1278
DOI 10.1007/s10544-009-9346-0

Triangular neuronal networks on microelectrode arrays: an approach to improve the properties of low-density networks for extracellular recording

Melanie Jungblut · Wolfgang Knoll · Christiane Thielemann · Mark Pottek

Published online: 15 September 2009

Abstract Multi-unit recording from neuronal networks cultured on microelectrode arrays (MEAs) is a widely used approach to achieve basic understanding of network properties, as well as the realization of cell-based biosensors. However, network formation is random under primary culture conditions, and the cellular arrangement often performs an insufficient fit to the electrode positions. This results in the successful recording of only a small fraction of cells. One possible approach to overcome this limitation is to raise the number of cells on the MEA, thereby accepting an increased complexity of the network. In this study, we followed an alternative strategy to increase the portion of neurons located at the electrodes by designing a network in confined geometries. Guided settlement and outgrowth of neurons is accomplished by taking control over the adhesive properties of the MEA surface. Using microcontact printing a triangular two-dimensional pattern of the adhesion promoter poly-D-lysine was applied to the MEA offering a meshwork that at the same time provides adhesion points for cell bodies matching the electrode positions and gives frequent branching points for dendrites and axons. Low density neocortical networks cultivated under this condition displayed similar properties to random networks with respect to the cellular morphology but had a threefold higher electrode coverage. Electrical activity was dominated by periodic burst firing that could pharmacologically be modulated. Geometry of the network and electrical properties of the patterned cultures were reproducible and displayed long-term stability making the combination of surface structuring and multi-site recording a promising tool for biosensor applications.

Keywords Cell patterning · Neuronal networks · Microelectrode arrays · Microcontact printing · Cell-based Biosensors · Burst firing

M. Jungblut · W. Knoll · C. Thielemann · M. Pottek
Max Planck Institute for Polymer Research,
Ackermannweg 10,
55128 Mainz, Germany

C. Thielemann (✉)
Faculty of Engineering, University of Applied Science,
Würzburger Straße 45,
63743 Aschaffenburg, Germany
e-mail: thielemann@fh-aschaffenburg.de

M. Pottek
Department for Zoology, Technical University of Kaiserslautern,
Erwin-Schrödinger-Str. 13,
67663 Kaiserslautern, Germany

1 Introduction

Cultivation of cells in an artificial environment requires physicochemical modification of the substrate surface to create appropriate conditions for cell adhesion and growth. Therefore, the substrate is coated with proteins promoting cell attachment, cell growth, and long-term viability. Such hybrid systems of inorganic material and living cells can be used to study cellular processes *in vitro* and provide the basic principle for biosensors and prostheses.

Cultivation of electrogenic cells like neurons on microelectrode arrays (MEAs) allows the non-invasive and simultaneous recording of electrical activity from multiple sites of a cell culture (Gross et al. 1977). Therefore, MEAs are a promising tool to study information processing in developing and mature neuronal networks (Gross et al. 1995, 1997; Potter 2001; Stett et al. 2003; Hofmann and Bading 2007) and are also useful for biosensor applications

(Keefer et al. 2001; Chiappalone et al. 2003; Selinger et al. 2004; Martinoia et al. 2005; Xiang et al. 2007).

But growth of dissociated neurons on a homogeneously coated surface results in a random network formation, where cell adhesion often shows a sparse fit to the electrode positions of the MEA. A solution to improve cellular arrangement of low density cultures with respect to the geometry of the recording sites is to control the surface properties of the electronic device. Such guidance of cell adhesion and cell growth directs neuronal cell bodies to the electrodes and therefore fosters the successful extracellular recording of the neuronal activity by a MEA.

Topographical influence on growth and network formation of cultured neurons has been exerted by a number of approaches including surface texture manipulation (Curtis and Wilkinson 1997) and patterned deposition of adhesion promoting proteins (Wheeler et al. 1999; Scholl et al. 2000; Nam et al. 2004). For the latter approach, surface chemistry based on silane- or alkanethiol self-assembled monolayers (SAMs) was applied to serve as linker for cell attractive or repulsive molecules. In contrast, microcontact printing offers a less intricate approach to achieve direct deposition of adhesion promoting proteins with high spatial resolution. Polydimethylsiloxane (PDMS) microstamps with a geometric pattern are used to transfer adhesion promoting molecules on substrate surfaces. Originally introduced for printing a pattern of alkanethiolates onto a gold substrate (Kane et al. 1999) this method has already been used to study patterned growth of neurons (Wheeler et al. 1999; Lauer et al. 2001; James et al. 2004; Chang et al. 2006; Jun et al. 2007). But these approaches showed that detection of signals from many recording sites and long-term maintenance of network structure still remains a challenge to be mastered for successful use of the system in a biosensor format.

Former attempts to control neuronal network formation *in vitro* were dealing with rectangular or striped patterns (Ma et al. 1998; Wheeler et al. 1999; Branch et al. 2000; Liu et al. 2000; Lauer et al. 2002; Vogt et al. 2003, 2005; James et al. 2004; Heller et al. 2005; Jun et al. 2007), which offer a rather untypical geometry for the more radially organized neuronal outgrowth *in vivo*.

In order to obtain a cellular morphology more similar to that observed in random two-dimensional cell growth, a triangular pattern of the adhesion promoter poly-D-lysine was applied. Intersection points of the pattern were adjusted to the electrode positions to serve as adhesion sites for the cells, while neurite outgrowth was directed along internodal lines. This patterning strategy allowed effective cell-electrode coupling and guiding of neuronal growth under reproducible surface conditions. Characterization of cellular morphology and electrophysiological properties showed that patterned neocortical networks maintained viability, functionality, and geometry over several weeks.

2 Materials and methods

2.1 Cell culture

Neocortical cells were obtained from rat fetuses at day 18 of gestation (E18). Pregnant CD rats were purchased from Charles River (Sulzfeld, Germany) and were sacrificed in accordance with the current German Animal Protection Law. All procedures were approved by the regional animal care and use committee (Landesuntersuchungsamt Rheinland-Pfalz, Germany). Fetuses were revealed by caesarean, decapitated, and transferred to ice-cold HBSS including 10 mM HEPES (Invitrogen, Germany) for removal of the brain. Meninges were peeled off, and frontal cortices were collected for cell extraction. Following incubation in medium containing cystein-activated papain (papain: 2 U/ml; L-cystein: 0.2 mg/ml; Sigma) and DNase I (300 U/ml; Roche) at 37°C for 30 min cortices were triturated using a set of Pasteur pipettes with progressively constricted opening diameters. The resulting cell suspension was then passed through a cell strainer (40 µm pore size; BD Biosciences, Heidelberg, Germany) and centrifuged (1,300 rpm, 4°C, 5 min). The pellet was re-suspended in serum-free B27/Neurobasal medium supplemented with 0.5 mM glutamine (Brewer et al. 1993; Brewer 1995), and density of living cells was determined by Trypan Blue exclusion.

Cells were seeded at a density of 200 cells mm^{-2} on surface-modified MEAs or glass cover slips and cultivated in a humidified atmosphere containing 5% CO_2 at 37°C. For electrophysiological control experiments with random cultures cells were plated at a density of 1,000 cells mm^{-2} to attain sufficient electrode coverage for recording of neuronal network activity. Medium renewal was performed twice a week. A culture dish lid made of a transparent and gas-tight FEP Teflon® (fluorinated ethylene propylene) membrane with selective permeability to oxygen and carbon dioxide served to reduce evaporation from the medium supply and at the same time prevented invasion of airborne contaminants (Potter and DeMarse 2001).

2.2 Microcontact printing

Patterned deposition of the cellular adhesion promoting agent poly-D-lysine (PDL) on MEA surfaces was performed by microcontact printing (Kane et al. 1999) using customized polydimethylsiloxane (PDMS) microstamps.

A master stamp providing the negative of the designated pattern was produced by photolithography using a chromium mask (Delta Mask, Enschede, the Netherlands) as template. Photoresist layers (AZ 9260; Clariant GmbH, Sulzbach, Germany) of 10 µm thickness were spin-coated on glass wafers and subsequently hard-baked at 100°C for

12 min. Structuring was done by exposure to UV irradiation while the mask was in close contact with the photoresist layer. From the resulting mold microstamps were cast after surface treatment with the anionic detergent sodium dodecyl sulfate (2% w/v, 5 min; Sigma) to facilitate later removal of the stamp. Casting was done by pouring the elastomeric polymer PDMS (Sylgard® 184; Dow Corning, Wiesbaden, Germany) into glass rings with a diameter of 5 mm on the master and subsequent overnight curing at 70°C. Stamps were then decontaminated in 70% ethanol for 30 s before they were soaked overnight in a sterile solution of 0.1 mg/ml PDL (70,000–150,000 MW; Sigma) in phosphate-buffered saline pH 8.0. Prior to use, microstamps were dried by a nitrogen airstream, optically adjusted to the electrode geometry of the MEA by means of a special stereomicroscope (Leica MS5, Leica Microsystems, Germany) combined with a fineplacer (Fineplacer-145 PICO, Finetech Electronics, Germany) and pressed to the MEA surface with a force of about 100 g/cm^2 for 15 min at room temperature.

Pattern geometry consisted of a grid of isosceles triangles with 4 or 6 µm line width, respectively, giving intersection points between three straight lines at a time and internodal distances of 100 µm at the base and 112 µm at the sides of the triangle. Nodes were arranged to match the electrode coordinates of the MEA leading to a situation with each third node being occupied by an electrode. This pattern was chosen to offer the neurons appropriate conditions for radial outgrowth and frequent branching of neurites in order to facilitate a cellular morphology similar to that obtained with unbiased conditions.

For control cultures, surfaces were homogenously treated with PDL to trigger accidental adhesion of cells leading to random network formation.

2.3 Immunocytochemistry

After 14 days *in vitro*, patterned and random cultures with a cell density of 200 cells mm^{-2} on cover slips were fixed with 4% paraformaldehyde in phosphate buffer (pH 7.4) for 20 min at 4°C. Unspecific binding sites were blocked by incubation with 5% normal donkey serum (Dianova, Hamburg, Germany) in phosphate-buffered saline (PBS) for 30 min at room temperature before cells were permeabilized with Triton X-100 (0.6% in PBS, 20 min, 4°C). Primary antibodies (rabbit polyclonal anti-MAP2 (Chemicon, 1:200), mouse monoclonal anti-MAP2a/2b (Abcam, 1.5 µg/ml), mouse monoclonal anti-GFAP (Chemicon, 1:400), mouse monoclonal anti-neurofilament 160 (Abcam, 1:200), rabbit polyclonal anti-synapsin (Abcam, 1:500)) were diluted in 1% normal donkey serum and 0.15% Tween-20 in PBS and applied overnight at 4°C. After rinsing with PBS, secondary antibodies raised in donkey were applied for 3–12 h with a dilution of 1:100 (rhodamine anti-rabbit IgG, Fluorescein isothiocyanate anti-rabbit IgG, rhodamine anti-mouse IgG, Fluorescein isothiocyanate anti-mouse IgG (Chemicon)). Control experiments with omitted primary antibodies resulted in the complete absence of any staining indicating no unspecific binding of the secondary antibodies. In case of double-labeling, antibody treatments were performed serially for the given antigens.

Cover slips were mounted on microscopic slides using fluorescence mounting medium (DakoCytomation, Carpinteria, CA, USA), and samples were analyzed by confocal microscopy using a Zeiss LSM 510 (Zeiss, Goettingen, Germany) equipped with an argon and helium/neon laser.

Fluorescent labeling was quantified using MetaMorph® (Molecular Devices, Downingtown, PA, USA). Labeled morphological features were extracted from the micrographs by intensity thresholding, and respective pixel number or labeled area was determined. Photographs were taken with a 40fold objective (pixel size: 0.23 µm×0.23 µm).

2.4 Electrical recording

Electrical activity was extracellularly recorded using a MEA60 setup (Multi Channel Systems, Reutlingen, Germany) consisting of a 60 channel amplifier and data acquisition card for conversion of analog signals to digital data streams. Data sampling was performed with a rate of 10 kHz. A thermal element maintained a culture medium temperature of 37°C during the experiments. Multielectrode arrays (MEA; Multi Channel Systems) consisted of 60 electrodes made of titanium nitride embedded in a glass substrate in an 8×8 array. Electrode diameters were 30 µm and inter-electrode spacing was 200 µm. Recorded signals (spikes) were displayed in real time using the software package MC_Rack (Multi Channel Systems) and saved for offline analysis covering signal detection, waveform sorting, and signal rate determination which was performed with the same software.

Occurrence of bursts in the spike pattern was detected by a custom-made application written in Java® based on an analysis of consecutive interspike intervals (Tam 2002; Chiappalone et al. 2005). For burst detection the following criteria were chosen: *(i)* Interspike intervals at burst onset should not exceed 10 ms; *(ii)* a burst should consist of at least 3 spikes; *(iii)* after the third spike, interspike intervals of maximally 20 ms were tolerated reflecting the observation of increasing interspike intervals with burst duration; *(iv)* intervals between consecutive bursts should last for more than 500 ms. Otherwise, respective spike barrages were considered a single burst.

Test substances (Bicuculline methiodide, GABA; Sigma) were dissolved in culture medium and were manually applied by bulk exchange.

2.5 Statistics

Data (given as mean ± standard deviation of *n* samples) was collected from different cell cultures. For quantitative analysis of the immunostaining results 6 micrographs were taken from every culture. Mean values of the samples were compared statistically by using either Student's t-test for normally distributed values or Mann–Whitney U test as a non-parametric test. Differences were considered statistically significant for $P<0.05$.

Data points of dose-response curves for electrophysiological recordings were fitted by using the logistic function $y = A_2 + [A_1–A_2 / (1 + (c/c_0)\text{^}(n_H))]$ where c donates the concentration of the test substance, c_0 the half maximal effective concentration (designated as EC_{50} for excitation and IC_{50} for inhibition), n_H the Hill coefficient, and A_1 and A_2 the burst rate under control conditions and following a saturating concentration of the test substance.

3 Results

3.1 Cell growth of patterned neuronal networks

Surface patterning of poly-D-lysine (PDL) resulted in a clear triangular network structure, and cell adhesion as well as growth followed the pattern reliably. The PDL-coating promoted adhesion of cell bodies and stellate neurite outgrowth, whereas uncoated areas were not overgrown by neurites and were almost devoid of cell bodies.

For comparison of cell growth on electrodes in structured and in non-manipulated networks, cells were seeded with a density of 200 cells mm^{-2} on a MEA surface that was either homogeneously coated with PDL or printed with a triangular pattern of 6 µm wide PDL lines.

Neurons cultured on patterned surfaces assembled into an ordered network with cell bodies confined to the nodes of the meshwork and neurites extending along the predefined internodal lines. As the nodal intersection points were arranged to match the electrode coordinates of the MEA, the triangular PDL pattern promoted cell adhesion at the electrode positions while the homogeneously coated surfaces resulted in random electrode coverage (Fig. 1(a) and (b)).

Quantitative analysis showed that the number of occupied electrodes was almost three times higher for patterned networks in comparison to random network formation (Fig. 1(c)). In average 28 electrodes were covered by neuronal cell bodies for patterned cell growth, whereas cell bodies were located on just 11 electrodes in case of random networks. This result shows that patterning is a suitable method to increase the portion of neuronal cell bodies coupled to electrodes for networks of low cell densities.

3.2 Morphological characterization of patterned neuronal networks

To determine whether guided cell growth was associated with major alterations in cellular organization, parameters as astroglial growth, neurite elongation, and synaptic density were analyzed by immunostaining.

Growth of astrocytes, which are known to promote synaptogenesis and synaptic efficiency (Pfrieger and Barres 1997), was assessed by immunocytochemical staining of glial fibrillary acidic protein (GFAP), an intermediate filament of the astroglial cytoskeleton. Due to the thin lines forming the pattern, astrocytes showed a rather slim morphology of the cell body in comparison to cells on homogeneously coated surfaces (Fig. 2(a) and (b)). The area labeled by antibody staining of GFAP was analyzed to compare astrocyte growth on patterned and homogeneously

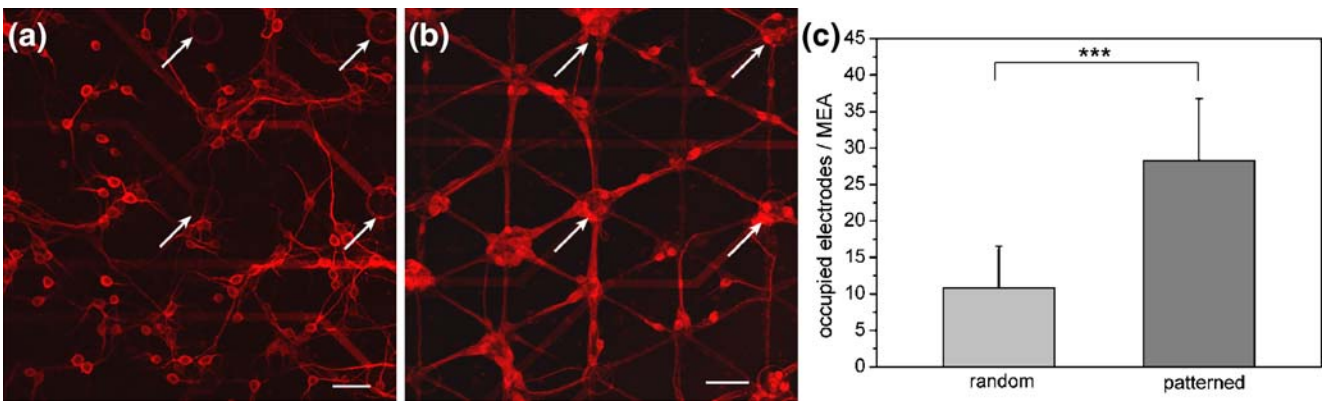

Fig. 1 Neuronal cell cultures on microelectrode arrays (a, b) Labeling of neuronal cell bodies and dendrites using an antibody directed against MAP-2 for random (**a**) and patterned (**b**) networks (line width: 6 µm) at 7 div. Some electrodes are highlighted by arrows. Scale bars, 50 µm. (**c**) Average number of electrodes covered by neuronal cell bodies for random and patterned cell growth at 7 div (n=12; *** $P<0.001$)

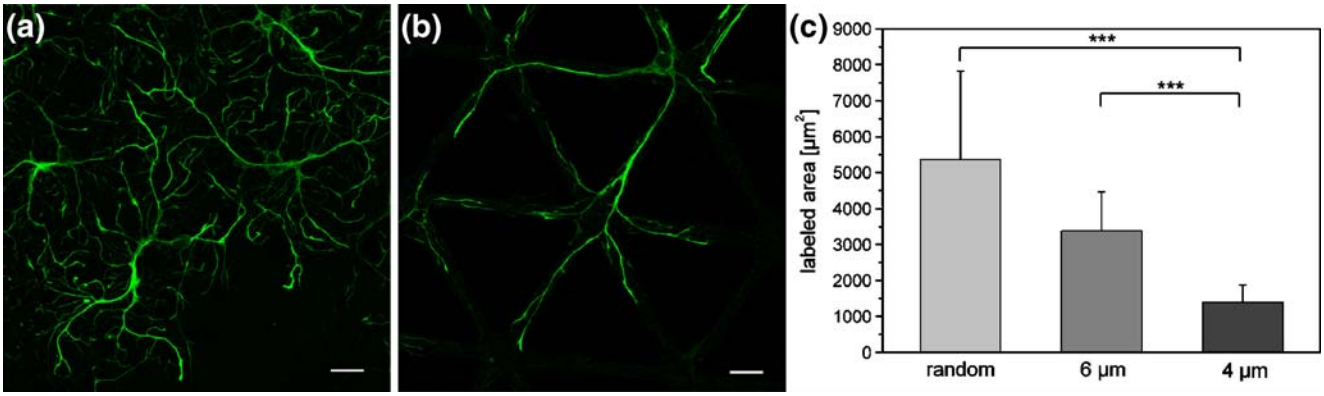

Fig. 2 Astrocyte growth for different culture conditions (a, b) Astrocytes were labeled by antibody staining of GFAP in random (**a**) and patterned (**b**) networks at 14 div. Staining of astrocytes in networks with 4 µm wide lines is not shown as almost no staining was present in these cultures. Scale bars, 20 µm. (**c**) Average labeled area per picture of GFAP-positive structures at 14 div (n=60; *** P<0.001)

coated substrate surfaces. Some astrocytes were detected after 7 days *in vitro* (div), whereas the number increased substantially within the second week *in vitro* but remained at a constant level thereafter (Fig. 2(c)). The average GFAP-labeled area of random networks after 14 div is slightly higher in comparison to structured networks with 6 µm wide lines, though this difference was not significant. But cultures showed a very low number of GFAP positive cells when a pattern with 4 µm line width was applied resulting in a significantly (P<0.001) reduced GFAP-labeled area compared to random cultures and networks on 6 µm wide lines.

Examination of axonal growth was done by immunostaining of Neurofilament (160 kD), a protein of the axonal cytoskeleton, after 2 and 3 weeks *in vitro* (Fig. 3(a) and (b)). Evaluation of the average pixel number of Neurofilament-positive structures showed a considerable increase between the second and third week *in vitro*, demonstrating remarkable cell growth and interneuronal wiring during this period (Fig. 3(c)). Moreover, surface patterning did not constrict axonal outgrowth. Rather, there was a slight increase of Neurofilament-positive structures after 14 div in patterned cultures that may reflect an accelerated axonal elongation due to easy path-finding when following the predetermined PDL-lines.

Development of synapse formation was assayed by double-immunostaining for MAP-2 and Synapsin I, a presynaptic marker protein, for random and patterned networks after 7, 14 and 21 div (Fig. 3(d) and (e)). For quantitative analysis, pixel number of Synapsin I positive cellular structures per neuron was analyzed. Synapsin I immunoreactivity could be detected after 7 div in both network types (Fig. 3(f)). The pixel number of synapsin-labeled structures increased threefold within the second week *in vitro*, and remained constant thereafter. Compared to random cultures patterned neuronal networks displayed a similar profile of synaptic density with culture time (Fig. 3(f)) leading to the assumption that synaptogenesis is not adversely affected by surface patterning.

3.3 Electrophysiological properties of patterned neuronal networks

3.3.1 Spontaneous electrical activity

Spontaneous activity of patterned networks with 6 µm line width growing on MEAs could be discerned after 10 div in terms of single spikes representing neuronal action potentials. Following two weeks of cultivation, spike trains exhibited increased signal density. Furthermore, as a prominent temporal feature of the activity, so-called bursts were displayed after two weeks *in vitro*. These barrages of spikes occurred with high synchronicity between different recording sites and were even recorded from sites that were otherwise silent (Fig. 4(a)). Within the third week *in vitro*, burst firing stabilized to a robust and regular pattern of 3–6 bursts per minute. Burst duration was 100–150 ms, with a spike frequency of approximately 150 Hz. Each burst was followed by a silent period of at least 0.5 s (Fig. 4(b)).

Spikes could be detected with a very high signal-to-noise ratio that exceeded 5:1 (Fig. 4(a) and (b)). Individual spikes typically displayed a negative component of 50–100 µV amplitude with maximal values of 200–300 µV followed by a less pronounced positive component of 10–50 µV amplitude with maximal values of 50–100 µV. Using the spike sorting tool implemented in the MC_Rack software, signals originating from different neurons on one given electrode were discriminated by waveform dissimilarity that arises from differences in cell-electrode coupling and cell body diameter (not shown). In these recordings, signals were attributed to 1–2 neurons per electrode. Quantitative analysis showed that spike trains could be observed from about 25 of 60 electrodes of the MEA in patterned networks

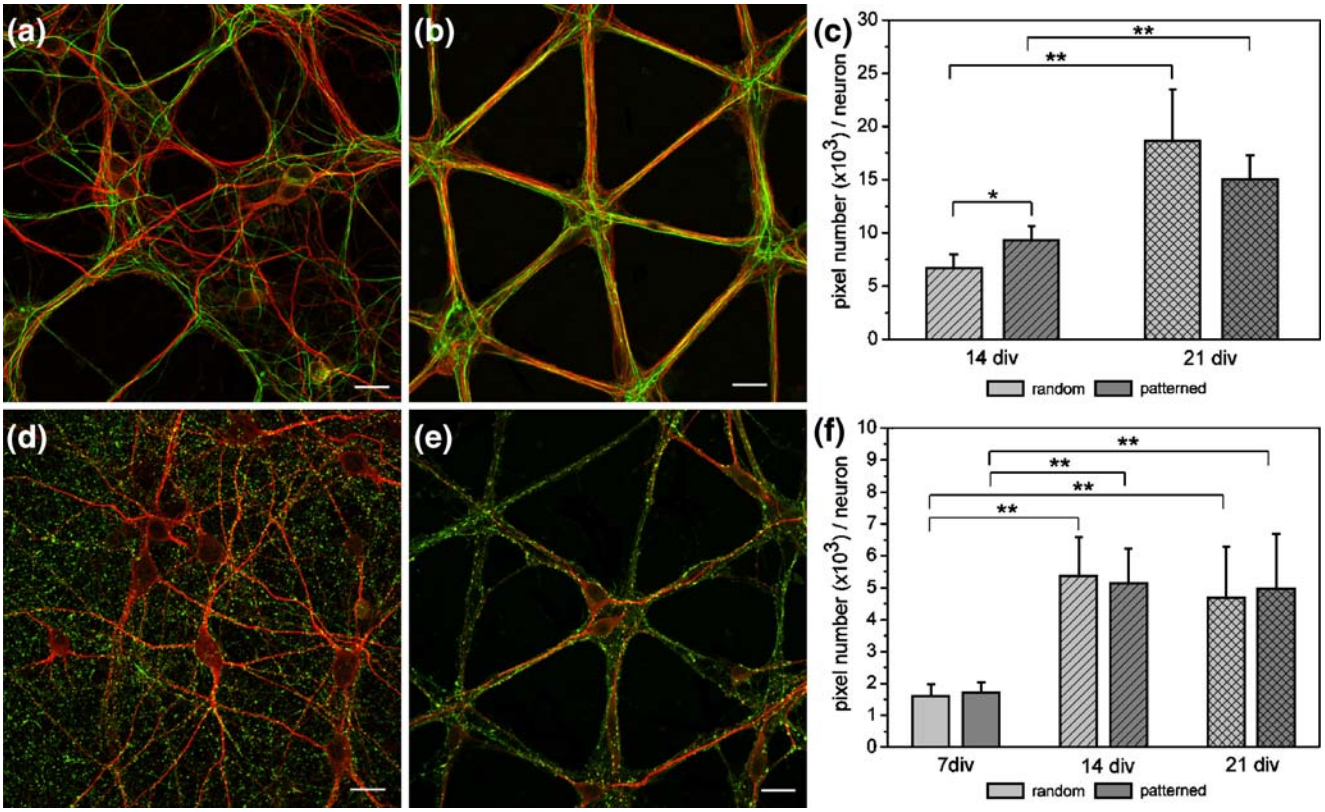

Fig. 3 Axonal growth and synaptic density in random and patterned neuronal networks (line width: 6 μm) (a, b) Fluorescence micrographs of neuronal networks showing axonal growth on homogeneously coated (**a**) and patterned substrate surfaces (**b**) at 14 div. MAP-2 positive cell bodies and dendrites are depicted in red. Axons were labeled by antibody staining against Neurofilament 160 kD (green). (**c**) Average pixel number of Neurofilament-positive structures per neuron at 14 and 21 div (n=30; * P<0.05; ** P < 0.01). (d, e) Fluorescence micrographs showing synaptic density in cultures after 14 div. Presynaptic sites in random **d** and patterned (**e**) networks were labeled by immunodetection of Synapsin I (green). Neuronal cell bodies and dendrites were labeled by MAP-2 immunoreactivity (red). (**f**) Average pixel number per neuron of Synapsin puncta at 7, 14 and 21 div (n=30; ** P<0.01). Scale bars, 20 μm

with 6 μm line width (Fig. 4(c)). In contrast, random network formation by low cell density cultures resulted in successful recording of electrical activity from just 10 electrodes.

Electrophysiological measurements, which were performed with patterned networks of 4 μm line width, revealed that these cultures did not show any burst activity. The activity pattern of these networks consisted only of single spikes without any synchronicity between different recording sites. Consequently, only networks cultivated on 6 μm wide PDL-lines were used for further electrophysiological recordings.

3.3.2 Network response to neuroactive agents

Treatment with the neuroactive substances GABA and Bicuculline was performed to verify whether the reaction of patterned networks was physiologically reasonable and comparable to that of random networks. As low density random cultures (200 cells mm^{-2}) showed only poor electrode coverage and were not suitable for electrophysiological measurements, plating density was increased (1,000 cells mm^{-2}) to attain sufficient electrode coverage for electrical recording. In contrast, patterned cultures were used with a density of 200 cells mm^{-2}. Measurements were performed within the third week of cultivation when burst firing stabilized to a robust and regular pattern. Bursts as the predominant feature of the activity pattern were chosen as parameter for the quantitative analysis of electrical activity. These high frequency barrages of action potentials are a key phenomenon in cortical neuronal networks *in vitro* (Maeda et al. 1995; Jimbo and Robinson 2000) and are supposed to be caused by a lack of sensory inputs (Waagenar et al. 2005). Bursts were described as an adequate tool to analyze spontaneous activity in cortical cultures (Kamioka et al. 1996; Chiappalone et al. 2005; Waagenar et al. 2006; Raichman and Ben-Jacob 2008).

GABA application resulted in a dose-dependent decrease in burst rate (Fig. 5(a)) and spike rate (not shown). The IC_{50} for the inhibition of burst activity was 1.63±0.14 μM (n=3) for patterned cultures and close to that of random networks (IC_{50} = 1.43±0.11 μM). A GABA concentration of 10 μM resulted in a total inhibition of firing.

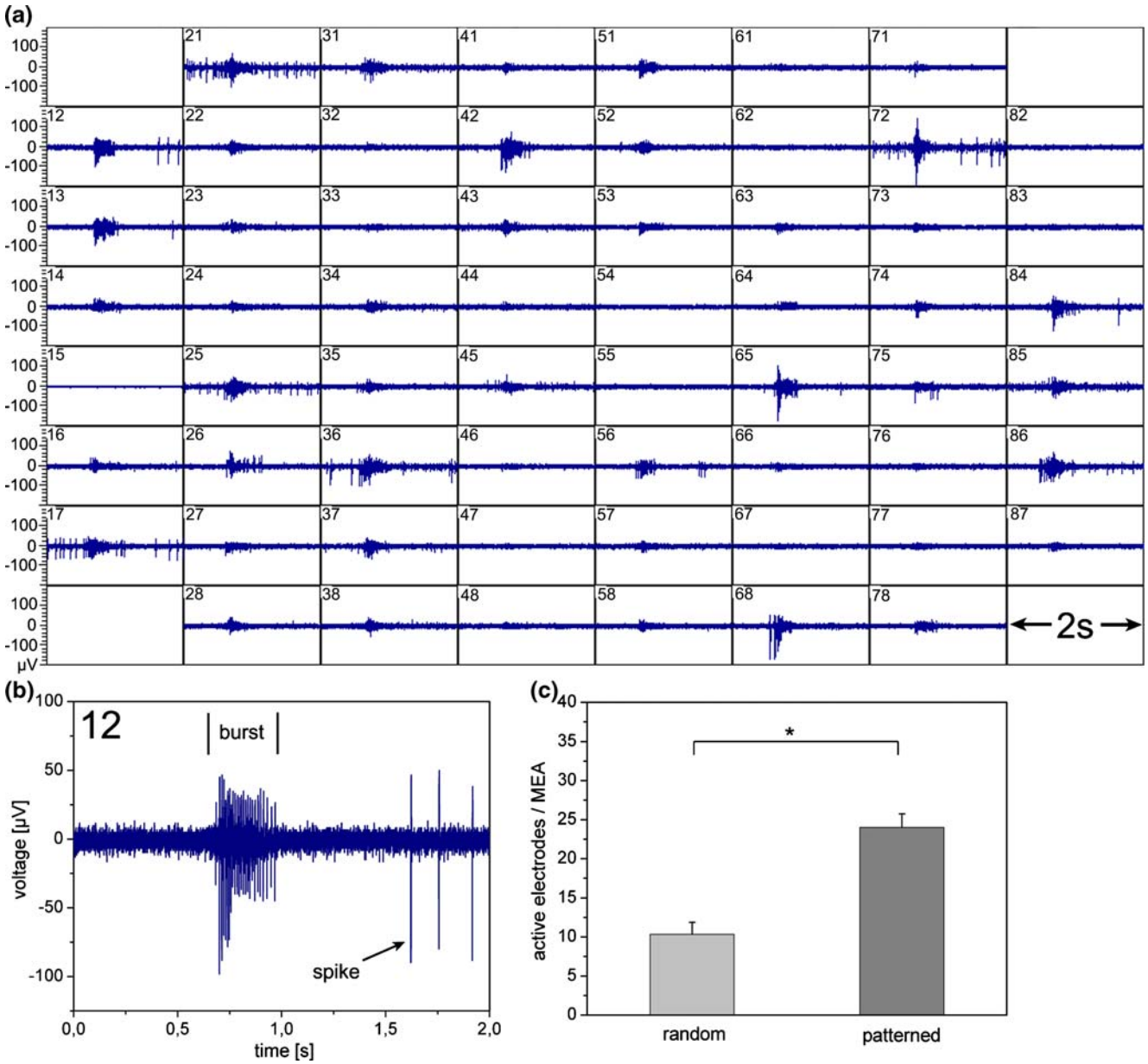

Fig. 4 Spontaneous electrical activity of mature patterned networks (line width: 6 µm) (**a**) Electrical activity recorded by the 60 electrodes of a MEA at 24 div. The activity pattern shows single spikes and one burst. Bursts occur synchronized at several electrodes. (**b**) Neuronal activity detected by electrode 12. Every burst is followed by a silent period of at least 0.5 s before single spikes are observed again. (**c**) Average number of electrodes detecting neuronal electrical activity for random and patterned networks after 24 div (n=3; * P<0.05)

The $GABA_A$-receptor antagonist Bicuculline was applied in a concentration range of 0.01–5 µM (Fig. 5(b)). The burst rate increased substantially and the network activity was dominated by a regular pattern of bursts synchronized over different channels. This observation was consistent with the convulsant activity of Bicuculline resulting from a disinhibition of the network from GABAergic activity. The EC_{50} was 0.77±0.11 µM and not significantly different to that of random networks (EC_{50} = 0.80±0.14 µM). Removal of the pharmacological agent was performed by complete medium change and resulted in a recovery of the reference activity within 10 min.

4 Discussion and conclusions

In this study, we present an approach to improve the properties of low-density patterned neocortical networks

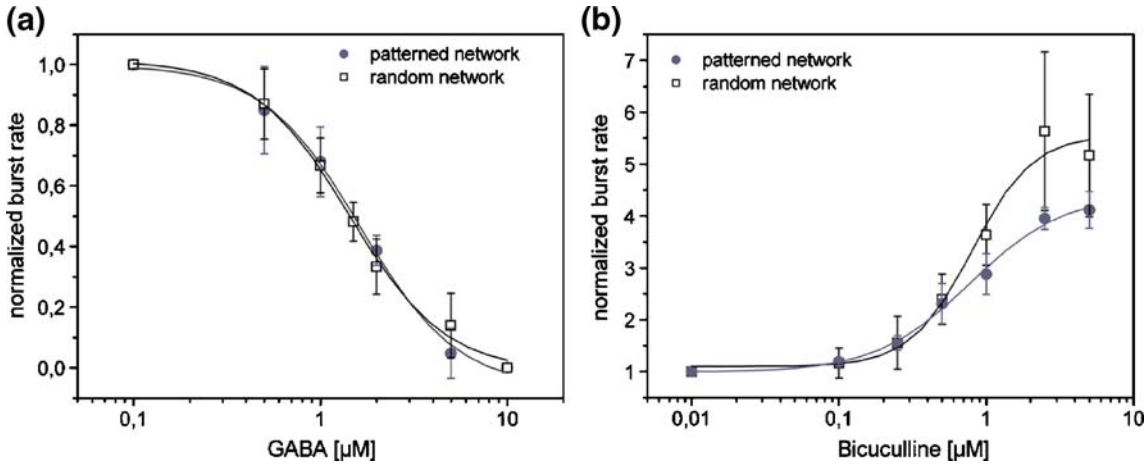

Fig. 5 GABAergic modulation of the network activity (**a**) Dose-response curve for GABA-mediated inhibition of spontaneous burst activity. The IC_{50} was 1.63 µM for patterned networks (line width: 6 µm) and 1.43 µM for random networks of high cell density (n=3). (**b**) Increase of spontaneous burst activity in response to the $GABA_A$-receptor antagonist Bicuculline. Bicuculline application resulted in an EC_{50} of 0.77 µM for patterned networks (line width: 6 µm) and 0.80 µM for random networks of high cell density (n=4)

cultivated on a microelectrode array chip with respect to a higher number of active electrodes, enhanced signal-to-noise ratio and reproducible electrophysiological properties. Pattern dimensions were adapted to the electrode geometry of the chip and permitted controlled cell adhesion at the electrode positions, enhanced reproducibility of network formation and effective cell-electrode coupling. In average, electrical activity could be detected from almost 50% of the electrodes, and networks showed robust and reproducible activity for at least four weeks *in vitro*.

Microcontact printing (Kane et al. 1999) was used to create a pattern of the adhesion promoter poly-D-lysine on the MEA surface. Binding of poly-D-lysine to the silicon nitride surface of the MEA by electrostatic interaction was stable for several weeks and opposing to other studies no further surface chemistry was required (Ma et al. 1998; Wheeler et al. 1999; Branch et al. 2000, 2001; Lauer et al. 2002; Chang et al. 2003; Nam et al. 2004).

Triangular pattern geometry promoted cell adhesion at the intersection nodes, which were arranged to match the electrode positions, and offered appropriate conditions for stellate neurite outgrowth. In contrast to rectangular or striped patterns used in former studies (Ma et al. 1998; Wheeler et al. 1999; Branch et al. 2000; Liu et al. 2000; Chang et al. 2001; Lauer et al. 2002; Vogt et al. 2003, 2005; Heller et al. 2005; Chang et al. 2006; Jun et al. 2007) the triangular geometry triggered a cellular morphology more similar to random cell growth and promoted efficient branching of the neurons which resulted in an at least 4 times higher number of active electrodes in comparison to previous observations (James et al. 2004; Nam et al. 2004; Jun et al. 2007). Furthermore, effective coupling of the neurons to the electrodes led to substantial improvement in signal-to-noise ratio with spike amplitudes of usually more than 100 µV peak to peak. Highly synchronized bursts, known to be a key phenomenon in random cortical networks, were detected from cultures of patterned networks and identified as an apparent and robust feature of the activity pattern. The occurrence of bursts indicates that synaptic inputs are reliably transmitted by neurons and that synaptic connections are functional in these networks (Maeda et al. 1995).

Furthermore, the physiologically relevant and reproducible modification of spontaneous neuronal burst activity by application of the inhibitory neurotransmitter GABA and the $GABA_A$-receptor antagonist Bicuculline was demonstrated. Application of GABA caused a dose-dependent decrease in burst activity, while the convulsant drug Bicuculline led to a disinhibition of the network activity. Such reproducible modification of neuronal activity is not only important to confirm the functionality of the network, but also demonstrates the usefulness of patterned neuronal networks on MEAs as cell-based biosensors. In this context, sparse networks of defined architecture can be used to monitor biochemical modification of electrical activity on the single cell as well as on the network level.

Immunostaining assays and electrical recording showed that morphological and electrophysiological properties of patterned cultures kept up with those of random networks. Consistent with previous studies (Ma et al. 1998; Liu et al. 2000) it was shown that synapse formation in patterned networks is comparable to that among neurons grown under non-manipulated conditions. Such proper development of synapses and neurites is crucial for functional networks. Increase of Synapsin I immunoreactivity within the second week *in vitro* was correlated to the appearance of bursts, which indicates functional synaptic connectivity at this time.

An important feature for neuronal survival, appropriate synaptogenesis and functionality of a neuronal network is

the presence of astrocytes (Pfrieger 2002; Ullian et al. 2004; Boehler et al. 2008). The results showed that synapse density increased simultaneously with astrocyte density within the second week *in vitro*. Also, the appearance of bursts after two weeks *in vitro* was correlated to an increase in the number of astrocytes, suggesting that astrocytes are important for synaptogenesis and synaptic efficacy (Pfrieger and Barres 1997; Christopherson et al. 2005).

The occurrence of synchronous bursts might also be supported by astroglial release of neuroactive molecules. Several studies showed that astrocytes have the ability to release glutamate and ATP (Angulo et al. 2004; Fellin et al. 2004, 2006; Carmignoto and Fellin 2006; Jourdain et al. 2007) which influences neuronal excitability, enhances synaptic strength and mediates synchronization of neuronal activity. The observation that networks plated on a PDL pattern with 4 μm line width comprise very few astrocytes together with an absence of burst firing also accounts for astrocytes playing a crucial part in the development of functional neuronal networks. These results also illustrate the importance of the pattern line width for the development and performance of the network. In a former study (Chang et al. 2006) astrocyte proliferation was even enhanced in patterned cultures. However, a pattern geometry composed of 40 μm wide lines was used which probably led to differences in network development and properties.

The current study illustrates a successful approach to combine neuronal patterning and multi-site recording by improving the properties of so far used rectangular patterned networks on a microelectrode array chip. The triangular network geometry imitates natural neuronal outgrowth and allows generation of low-density patterned networks with high electrode coverage and reliable morphological as well as electrophysiological properties. Sparse neuronal networks with defined geometry growing on MEAs are not only a promising tool for biosensor applications, but can also be used to gain fundamental understanding of activity-dependent neural network development and neuron-neuron as well as neuron-surface interactions.

Acknowledgments The authors thank Paul Kujawski for development of a burst detection software and Carmen Schwind for technical assistance.

References

C.M. Angulo, A.S. Kozlov, S. Charpak, E. Audinat, J. Neurosci. **27**, 6920 (2004)
M.D. Boehler, B.C. Wheeler, G.J. Brewer, Neuron Glia Biol. **3**, 127 (2008)
D.W. Branch, B.C. Wheeler, G.J. Brewer, D.E. Leckband, IEEE Trans. Biomed. Eng. **47**, 290 (2000)
D.W. Branch, B.C. Wheeler, G.J. Brewer, Biomaterials **22**, 1035 (2001)
G.J. Brewer, J.R. Torricelli, E.K. Everge, P.J. Price, J. Neurosc. Res. **35**, 567 (1993)
G.J. Brewer, J. Neurosc. Res. **42**, 74 (1995)
G. Carmignoto, T. Fellin, J. Physiol. Paris **99**, 98 (2006)
J.C. Chang, G.J. Brewer, B.C. Wheeler, Biosens. Bioelectron. **16**, 527 (2001)
J.C. Chang, G.J. Brewer, B.C. Wheeler, Biomaterials **24**, 2863 (2003)
J.C. Chang, G.J. Brewer, B.C. Wheeler, J. Neural Eng. **3**, 217 (2006)
M. Chiappalone, A. Vato, M.B. Tedesco, M. Marcoli, F. Davide, S. Martinoia, Biosens. Bioelectron. **18**, 627 (2003)
M. Chiappalone, A. Novellino, I. Vajda, A. Vato, S. Martinoia, J. van Pelt, Neurocomputing **65–66**, 653 (2005)
K.S. Christopherson, E.M. Ullian, C.C. Stokes, C.E. Mullowney, J.W. Hell, A. Agah, J. Lawler, D.F. Mosher, P. Bornstein, B.A. Barres, Cell **120**, 421 (2005)
A. Curtis, C. Wilkinson, Biomaterials **18**, 1573 (1997)
T. Fellin, O. Pascual, S. Gobbo, T. Pozzan, P.G. Haydo, G. Carmignoto, Neuron **43**, 729 (2004)
T. Fellin, O. Pascual, P.G. Haydon, Physiology (Bethesda) **21**, 208 (2006)
G.W. Gross, E. Rieske, G.W. Kreutzberg, A. Meyer, Neurosci. Lett. **6**, 101 (1977)
G.W. Gross, B.K. Rhoades, H.M.E. Azzazy, M.C. Wu, Biosens. Bioelectron. **10**, 553 (1995)
G.W. Gross, A. Harsch, B.K. Rhoades, W. Göpel, Biosens. Bioelectron. **12**, 373 (1997)
D.A. Heller, V. Garga, K.J. Kelleher, T. Lee, S. Mahbubani, L.A. Sigworth, R. Lee, M.A. Rea, Biomaterials **26**, 883 (2005)
F. Hofmann, H. Bading, J. Physiol. (Paris) **99**, 125 (2007)
C.D. James, A.J.H. Spence, N.M. Dowell-Mesfin, R.J. Hussain, K.L. Smith, H.G. Craighead, M.S. Isaacson, S. Shain, J.N. Turner, IEEE Trans. Biomed. Eng. **51**, 1640 (2004)
Y. Jimbo, H.P.C. Robinson, Bioelectrochemistry **51**, 107 (2000)
P. Jourdain, L.H. Bergersen, K. Bhaukaurallzy, P. Bezzi, M. Santello, M. Domercq, C. Matute, F. Tonello, V. Gundersen, A. Volterra, Nat. Neurosci. **10**, 271 (2007)
B.S. Jun, M.R. Hynd, N. Dowell-Mesfin, K.L. Smith, J.N. Turner, W. Shain, S.J. Kim, J. Neurosci. Meth. **160**, 317 (2007)
H. Kamioka, E. Maeda, Y. Jimbo, H.P.C. Robinson, A. Kawana, Neurosci. Lett. **206**, 109 (1996)
R.S. Kane, S. Takayama, E. Ostuni, D.E. Ingber, G.M. Whitesides, Biomaterials **20**, 2363 (1999)
E.W. Keefer, A. Gramowski, D.A. Stenger, J.J. Pancrazio, G.W. Gross, Biosens. Bioelectron. **16**, 513 (2001)
A. Lauer, C. Klein, A. Offenhaeusser, Biomaterial **22**, 1925 (2001)
L. Lauer, A. Vogt, C.K. Yeung, W. Knoll, A. Offenhaeusser, Biomaterials **23**, 3123 (2002)
Q.Y. Liu, M. Coulombe, J. Dumm, K.M. Shaffer, A.E. Schaffner, J.L. Barker, J.J. Pancrazio, D.A. Stenger, W. Ma, Dev. Brain Res. **120**, 223 (2000)
W. Ma, Q. Liu, D. Jung, P. Manos, J.J. Pancrazio, A.E. Schaffner, J.L. Barker, D.A. Stenger, Dev. Brain Res. **111**, 231 (1998)
E. Maeda, H.P.C. Robinson, A. Kawana, J. Neurosc. **15**, 6834 (1995)
S. Martinoia, L. Bonzano, M. Chiappalone, M. Tedesco, M. Marcoli, G. Maura, Biosens. Bioelectron. **20**, 2071 (2005)
Y. Nam, J.C. Chang, B.C. Wheeler, G.J. Brewer, IEEE Trans. Biomed. Eng. **51**, 158 (2004)
F.W. Pfrieger, B.A. Barres, Science **277**, 1684 (1997)
F.W. Pfrieger, Curr. Opin. Neurobiol. **12**, 486 (2002)
S.M. Potter, Prog. Brain Res. **130**, 49 (2001)
S.M. Potter, T.B. DeMarse, J. Neurosci. Meth. **110**, 17 (2001)
N. Raichman, E. Ben-Jacob, J. Neurosci. Meth. **170**, 96 (2008)

M. Scholl, C. Sproessler, M. Denyer, M. Krause, K. Nakajima, A. Maelicke, W. Knoll, A. Offenhaeusser, J. Neurosci. Meth. **104**, 65 (2000)
J.V. Selinger, J.J. Pancrazio, G.W. Gross, Biosen. Bioelectron. **15**, 675 (2004)
A. Stett, U. Egert, E. Guenther, F. Hofmann, T. Meyer, W. Nisch, H. Haemmerle, Anal. Bioanal. Chem. **377**, 486 (2003)
D.C. Tam, Neurocomputing **44–46**, 1155 (2002)
E.M. Ullian, K.S. Christopherson, B.A. Barres, Glia **47**, 209 (2004)
A.K. Vogt, L. Lauer, W. Knoll, A. Offenhaeusser, Biotechnol. Prog. **19**, 1562 (2003)
A.K. Vogt, G.J. Brewer, A. Offenhaeusser, Tissue Eng. **11**, 1757 (2005)
D.A. Waagenar, R. Madhavan, J. Pine, S.M. Potter, J. Neurosci. **25**, 680 (2005)
D.A. Waagenar, J. Pine, S.M. Potter, BMC Neurosci. (2006) doi:10.1186/1471-2202-7-11
B.C. Wheeler, J.M. Corey, G.J. Brewer, D.W. Branch, J. Biomech. Eng. **121**, 73 (1999)
G. Xiang, L. Pan, L. Huang, Z. Yu, X. Song, J. Cheng, W. Xing, Y. Zhou, Biosens. Bioelectron. **22**, 2478 (2007)